Journal of Biomechanics 47 (2014) 2904–2910

Contents lists available at ScienceDirect

Journal of Biomechanics

journal homepage: www.elsevier.com/locate/jbiomech
www.JBiomech.com

Pulmonary artery relative area change is inversely related to ex vivo measured arterial elastic modulus in the canine model of acute pulmonary embolization

Lian Tian [a], Heidi B. Kellihan [b], Joseph Henningsen [a], Alessandro Bellofiore [a], Omid Forouzan [a], Alejandro Roldán-Alzate [c], Daniel W. Consigny [c], McLean Gunderson [d], Seth H. Dailey [d], Christopher J. Francois [c], Naomi C. Chesler [a,*]

[a] Department of Biomedical Engineering, University of Wisconsin-Madison, 1550 Engineering Drive, Madison, WI 53706-1609, USA
[b] School of Veterinary Medicine, University of Wisconsin-Madison, 2015 Linden Drive, Madison, WI 53706-1102, USA
[c] Department of Radiology, University of Wisconsin-Madison, 600 Highland Avenue, Madison, WI 53792-3252, USA
[d] Department of Surgery, Division of Otolaryngology-Head and Neck Surgery, University of Wisconsin-Madison, 600 Highland Avenue, Madison, WI 53792-3252, USA

ARTICLE INFO

Article history:
Accepted 22 July 2014

Key words:
Pulmonary hypertension
Embolization
Elastic modulus
Relative area change

ABSTRACT

A low relative area change (RAC) of the proximal pulmonary artery (PA) over the cardiac cycle is a good predictor of mortality from right ventricular failure in patients with pulmonary hypertension (PH). The relationship between RAC and local mechanical properties of arteries, which are known to stiffen in acute and chronic PH, is not clear, however. In this study, we estimated elastic moduli of three PAs (MPA, LPA and RPA: main, left and right PAs) at the physiological state using mechanical testing data and correlated these estimated elastic moduli to RAC measured in vivo with both phase-contrast magnetic resonance imaging (PC-MRI) and M-mode echocardiography (on RPA only). We did so using data from a canine model of acute PH due to embolization to assess the sensitivity of RAC to changes in elastic modulus in the absence of chronic PH-induced arterial remodeling. We found that elastic modulus increased with embolization-induced PH, presumably a consequence of increased collagen engagement, which corresponds well to decreased RAC. Furthermore, RAC was inversely related to elastic modulus. Finally, we found MRI and echocardiography yielded comparable estimates of RAC. We conclude that RAC of proximal PAs can be obtained from either MRI or echocardiography and a change in RAC indicates a change in elastic modulus of proximal PAs detectable even in the absence of chronic PH-induced arterial remodeling. The correlation between RAC and elastic modulus of proximal PAs may be useful for prognoses and to monitor the effects of therapeutic interventions in patients with PH.

1. Introduction

Pulmonary hypertension (PH) is characterized by chronically high blood pressure in the pulmonary circulation. It is an important cause of morbidity and mortality in children and adults with over 10,000 deaths per year in US (Hyduk et al., 2005). Many metrics are used as prognostic indicators of PH such as pulmonary vascular resistance, pulmonary vascular input impedance, pulmonary vascular capacitance, pulmonary arterial (PA) compliance, PA stiffness, proximal PA relative area change (RAC), and various aspects of right ventricular (RV) function (Gan et al., 2007; Hunter et al., 2008; Mahapatra et al., 2006; Stevens et al., 2012; Swift et al., 2012). The proximal PA RAC is defined as the ratio of the change of PA area during a cardiac cycle and the PA area at diastole or systole. This metric was found by Gan et al. (2007) to be related to the mortality of patients with pulmonary arterial hypertension (PAH) and several more recent studies confirmed a strong correlation between this metric and mortality of patients with all-cause PH (Sanz et al., 2009; Stevens et al., 2012; Swift et al., 2012). Because RAC can be measured noninvasively, it is a promising metric for assessing disease progression and the effects of treatment.

As a normalized area change, i.e., essentially an area strain, however, RAC depends on the PA area at systole or diastole, the arterial wall thickness, and the arterial elastic modulus, all of which depend on the distending pressure, the latter because arteries are nonlinearly elastic (Kobs et al., 2005; Lammers et al., 2008; Wang et al., 2013). It is well known that proximal PA compliance and stiffness change significantly with PH progression

* Correspondence to: Department of Biomedical Engineering, University of Wisconsin-Madison, 2146 ECB, 1550 Engineering Drive, Madison, WI 53706-1609, USA.
E-mail address: chesler@engr.wisc.edu (N.C. Chesler).

http://dx.doi.org/10.1016/j.jbiomech.2014.07.013
0021-9290/

clinically (Mahapatra et al., 2006; Stevens et al., 2012) and basic science studies have shown that the increase in proximal PA elastic modulus with chronic PH is due to remodeling and changes in the extracellular matrix (Kobs et al., 2005; Lammers et al., 2008; Ooi et al., 2010). In acute PH such as can occur during exercise and with acute high-altitude or hypoxia exposure, the PA elastic modulus also increases due to the increase of pressure (Groves et al., 1987; Kornet et al., 1998; La Gerche et al., 2011; Motley and Cournand, 1947), although no arterial remodeling occurs. Understanding the correlation between RAC and elastic modulus would be clinically useful, because proximal PA stiffening impairs RV performance and is associated with RV dysfunction (Stevens et al., 2012).

The purpose of this study was to investigate the correlation between RAC and elastic modulus of proximal PAs. We did so using a model of acute PH, which has the advantage that the sensitivity of RAC to changes in elastic modulus can be assessed in the absence of chronic PH-induced remodeling. We first measured RAC in vivo using phase-contrast magnetic resonance imagining (PC-MRI) and 2D and M-mode transthoracic echocardiogrrarphy (Echo) both before and after creating of PH with acute embolization. After euthanasia, we obtained stress–stretch data ex vivo from uniaxial tensile testing. Then, we investigated the correlation between RAC and the calculated elastic modulus at physiological pressure. In addition, we examined if MRI and Echo imaging techniques can provide equivalent values of RAC.

2. Materials and methods

2.1. Animals and in vivo hemodynamic measurement

All experimental studies were performed after approval by the Institutional Animal Care and Use Committee. A total of 11 beagles were used in this study. Six adult female beagles (~1-year old) were used in acute pulmonary embolization study as described previously (Bellofiore et al., 2013). In these animals, after general anesthesia was induced by intravenous propofol injection (10 mg/kg body weight) and maintained with isoflurane (1–3% in 100% oxygen using mechanical ventilation), PC-MRI was performed to measure main, left and right PA (MPA, LPA and RPA) luminal cross-sectional areas and contrast-enhanced magnetic resonance (CE-MRA) was then performed to obtain the pulmonary vasculature images. Subsequently the dog was transferred to the catheterization lab, where it underwent Echo and right heart catheterization (RHC) to measure RPA inner diameter and PA pressures (PAPs) at baseline. Acute PH was then created by repeated injections of microbeads (Contour SE Microspheres, Boston Scientific, Natick, MA, USA) through the catheter in the right atrium until the mean PAP was greater than 30 mmHg, and then PAP measurements, Echo, and MRI without and with contrast were repeated. See references (Bellofiore et al., 2013; Roldán-Alzate et al., 2014) and Appendix A for detailed methods.

In five adult male beagles (~1-year old) with presumed normal pulmonary and RV function, 2D and M-mode Echo was performed to obtain RPA inner diameter of animals at rest. No acute pulmonary embolization was performed.

2.2. Ex vivo artery geometry measurement and mechanical tests

After animals were euthanized, intact proximal PAs were immediately harvested. After loose connective tissue was removed, the proximal PAs were soaked in calcium- and magnesium-free phosphate buffered saline at room temperature. Vessels were photographed ex vivo to measure the lengths of LPA and RPA without external load (Fig. 1B). Next, a short ring (~3 mm long) was obtained from each PA (MPA, LPA and RPA) and its cross-section was photographed. The ring was then cut once in the radial direction to obtain the stress-free or reference state and photographed again (Tian et al., 2011).

The cut-open arterial ring was taken as a circumferentially-oriented specimen for the uniaxial tensile test. A longitudinal specimen from MPA was not available; for LPA and RPA, longitudinal specimens were available in 5 and 8 animals, respectively. Both circumferential and longitudinal specimens were photographed to obtain thickness and width. The specimens were tested in an Instron 5548 MicroTester tensile testing system (Instron; Norwood, MA, USA) equipped with a 10 N load cell. Each specimen underwent ten uniaxial loading and unloading cycles with a constant strain rate of 20% length/s. To account for fluid forces or buoyancy against the test grips during testing, the specimen was then removed and one loading–unloading cycle was performed on the tensile testing system at the same strain rate to measure the buoyancy (Lopez-Garcia et al., 2010). Force–stretch data were obtained by subtracting buoyancy test data from the loading portion of the 10th cycle.

2.3. Data analysis

Proximal PA contours obtained from MRI were used to compute the luminal cross-sectional area at peak systole (A_{max}) and at end diastole (A_{min}). The minimal

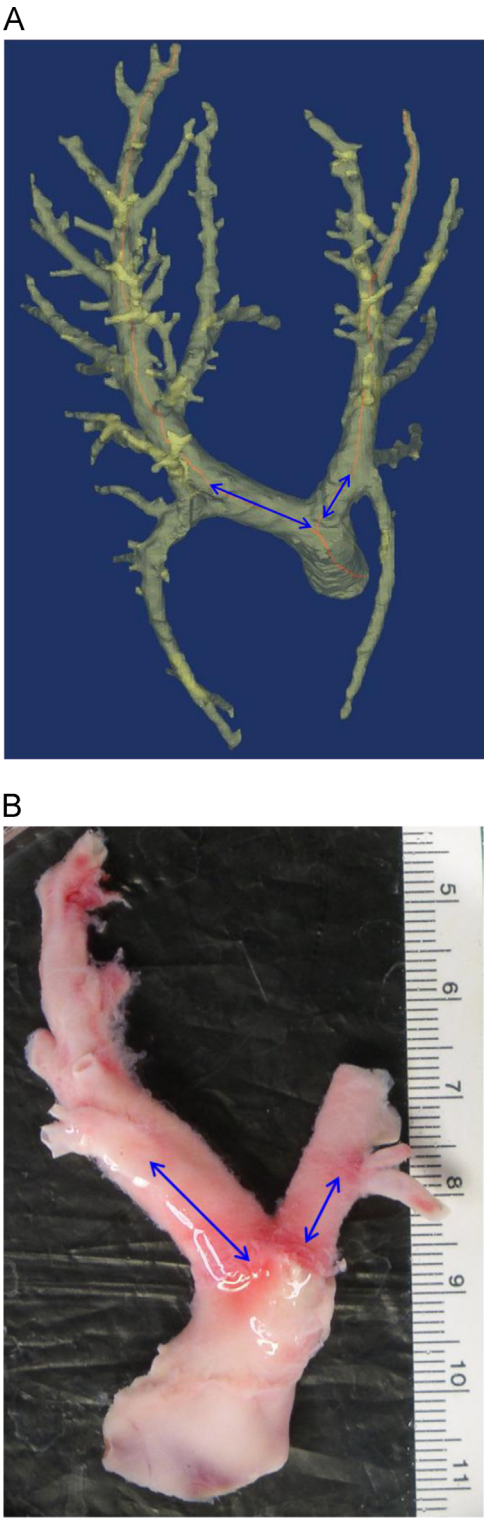

Fig. 1. Example of (A) in vivo and (B) ex vivo PA length measurement. The double arrows in both (A) and (B) indicates the length of LPA and RPA from the MPA bifurcation to the first branch from LPA and RPA, respectively. The red lines in (A) are the centerlines along the principal pulmonary arterial pathways.

and maximal inner diameters (ID_{min} and ID_{max}) were estimated by assuming a perfect circular shape, i.e., $A=\pi ID^2/4$. RPA ID_{min} and ID_{max} were also obtained from Echo and RPA A_{min} and A_{max} were estimated by $A=\pi ID^2/4$ given that the RPA cross section is quite close to circular from both in vivo MRI and ex vivo images. Relative area change (RAC) was defined as (Bellofiore et al., 2013)

$$RAC=\frac{A_{max}-A_{min}}{A_{max}}. \quad (1)$$

Here, the change of cross-sectional area is normalized by A_{max} rather than A_{min} because of the smaller error with normalization by A_{max} (see Appendix B).

To relate RAC to the ex vivo measured elastic modulus, we used the stress–stretch curve of the circumferential specimen measured from uniaxial tensile test and the estimated in vivo stress range, since RAC was measured in vivo. To estimate the in vivo stress range, the pressures at diastole and systole, the in vivo PA geometry and the reference geometry are required (Tian et al., 2012). In the six female animals, direct measurements of PAP were obtained by RHC; in the five male animals, PAPs in the pressure range of the female animals before embolization (9.2–17.5 mmHg; see Table 1) were assumed. The in vivo PA geometry was calculated based on the ex vivo proximal PA length and in vivo proximal PA length for animals on which CE-MRA was performed (Fig. 1). From the ex vivo image, we measured the length from the bifurcation of MPA to the middle of the next branch from LPA or RPA (Fig. 1B) as the ex vivo length of LPA or RPA, which is the reference length. In vivo proximal PA length was measured from CE-MRA images with Mimics (Materialise NV, Leuven, Belgium). Briefly, a threshold was visually chosen to create a mask for the pulmonary vasculature. PAs were then identified, distinct from pulmonary veins, by an observer blinded to condition, and centerlines along the principal pathways were calculated automatically by the software. The in vivo LPA and RPA length were measured along the centerlines from the MPA bifurcation point to the first distinctive branch point of LPA and RPA, respectively (Fig. 1A). The in vivo longitudinal stretch ratio for LPA or RPA was then estimated as

$$\lambda_z=\frac{L_z}{L_{z0}}, \quad (2)$$

where L_z and L_{z0} are the longitudinal lengths of LPA or RPA at in vivo and unloaded ex vivo, respectively. For MPA, there is no obvious marker close to the pulmonary valve either in the in vivo or ex vivo image for measuring MPA length. Therefore, we did not obtain λ_z for MPA. Rather, we assumed it was the same as LPA since geometrically MPA is aligned with LPA.

With the opened PA ring geometry (taken as reference state), λ_z, and ID_{min} or ID_{max} from MRI or Echo measurement, the incompressibility condition for artery allows us to calculate in vivo PA thickness at diastole or systole (Tian et al., 2012). The physiological stress range over which we calculated the elastic modulus was from the average circumferential stress (σ_θ) at diastole to σ_θ at systole, calculated under the thin-wall assumption (PA wall thickness-to-ID ratios at diastole were 0.09 ± 0.007 and 0.04 ± 0.003 before and after acute embolization, respectively). Specifically, σ_θ was calculated as

$$\sigma_\theta=\frac{P\cdot ID}{2h}, \quad (3)$$

where P is the diastolic or systolic PAP, and ID and h are the corresponding inner diameter and PA wall thickness at pressure P, respectively. Next, we used the physiological stress from Eq. (3) and found the corresponding stretch from the stress–stretch curve of the circumferential specimen tested ex vivo. A linear regression was then performed and the slope of the linear best fit to this physiological range was taken as the elastic modulus (E_{ex}).

With both RAC and E_{ex} calculated, we examined their relation assuming an inverse relationship of the form:

$$E_{ex}=\frac{A}{RAC}+B, \quad (4)$$

where A and B are the coefficients found from a linear regression between E_{ex} and 1/RAC.

2.4. Statistics

All data are presented as mean ± SD unless specified otherwise. Paired t-test was performed to compare PAP, λ_z, RAC, and E_{ex} before and after acute embolization, and RPA ID and RAC between MRI and Echo measurements. A two-tailed two-sample t-test was used to compare RPA RAC measured via Echo before ($n=11$) and after ($n=6$) acute embolization. Bland–Altman analysis (Bland and Altman, 1986) was used to assess the agreement between the two measurements of ID and RAC (MRI vs. Echo) and between RPA E_{ex} using in vivo RPA diameter measured via MRI and Echo. Simple linear correlations were determined between between E_{ex} and 1/RAC. $P<0.05$ was used to define statistical significance.

3. Results

PA pressure and cross-sectional area from MRI and RPA ID from Echo were obtained for all six female beagles before and after acute embolization. However, λ_z was obtained from only four of six female beagles because images of the ex vivo intact PA geometry (as in Fig. 1B) for two were not available. For those two female beagles as well as the five male beagles, which did not undergo MRI, we assumed LPA and RPA λ_z was the same as the measured average value of the other animals.

Hemodynamic data are summarized in Table 1. Acute embolization caused significant increases in PAP and λ_z of RPA but not LPA. With acute embolization, RAC measured via MRI decreased significantly in both MPA and LPA but not in RPA. RAC measured via Echo did not decease significantly in RPA when data from only the six female beagles was considered. However, when the five male beagles were included, RAC measured via Echo decreased significantly with acute embolization.

The RPA RAC measured via Echo agreed well with that measured via MRI (Fig. 2). The Echo measurement had a bias of −0.024 with limits of agreement of 0.30.

A representative stress–stretch curve is shown in Fig. 3. Before embolization, the physiological region is at low stretch with low elastic modulus, while after embolization, the region is shifted to higher stretch range with higher elastic modulus. Acute embolization-induced PH caused significant change in in vivo geometric data (PA systolic and diastolic IDs) measured from either MRI or Echo, leading to significant increase in E_{ex} (Fig. 4). Moreover, in vivo ID from Echo measurement was significantly smaller than that from MRI measurement (Fig. 5A; $P<0.002$), and this yielded significantly different elastic modulus of RPA (E_{ex}) between MRI and Echo measurement. Bland–Altman analysis found that the calculated E_{ex} using Echo geometry had a bias of −121 kPa with the limits of agreement of 291 kPa compared with that using MRI geometry (Fig. 5B). E_{ex} was consistently underestimated using Echo geometry and this underestimation was less in the absence of acute embolization-induced PH.

Moderate to strong linear correlations between elastic modulus and the inverse of RAC were observed for all three PAs (Fig. 6). The correlation for RPA RAC measured via Echo is slightly better than that for RPA RAC measured via MRI (Fig. 6E and F vs. Fig. 6C).

Table 1
Summary of pulmonary artery pressure, in vivo longitudinal stretch of LPA and RPA, and relative area change (RAC) of all three PAs before (PRE) and after (POST) acute embolization.

Parameter	PRE	POST	P-value
mPAP (mmHg)	13.0 ± 2.2	36.0 ± 8.7	< 0.001
sPAP (mmHg)	17.5 ± 2.5	48.7 ± 14.8	0.003
dPAP (mmHg)	9.2 ± 2.9	28.5 ± 5.7	< 0.001
LPA λ_z	1.11 ± 0.03	1.21 ± 0.08	0.10
RPA λ_z	1.32 ± 0.07	1.51 ± 0.09	0.003
MPA RAC	0.40 ± 0.05	0.25 ± 0.08	0.025
LPA RAC	0.52 ± 0.09	0.30 ± 0.04	0.008
RPA RAC	0.44 ± 0.11	0.36 ± 0.10	0.33
RPA RAC-Echo	0.46 ± 0.09	0.32 ± 0.12	0.12
RPA RAC-Echo-All	0.53 ± 0.13	0.32 ± 0.12	0.004

$n=4$–6 per group except that $n=11$ for RPA RAC measured with Echo before acute embolization. mPAP, sPAP, and dPAP, mean, systolic and diastolic pulmonary artery pressures, respectively; λ_z, in vivo longitudinal stretch. Pressure data were obtained from right heart catheterization (RHC) on six female beagles, and in vivo longitudinal stretch data are from four of these six female beagles. The data for "RPA RAC-Echo" only includes six female beagles, while the data for "RPA RAC-Echo-All" includes all the beagles.

4. Discussion

The relative area change (RAC) of proximal PAs has been found to be an excellent predictor of mortality in patients with PH in clinical studies (Gan et al., 2007; Stevens et al., 2012; Swift et al., 2012). However, what properties in the pulmonary circulation RAC is related to remain elusive. In this study, we investigated the relationship between RAC and elastic modulus using an adult canine model of acute PH so that we could assess the sensitivity of RAC to changes in elastic modulus in the absence of chronic PH-induced remodeling. We quantified proximal PA elastic modulus based on stress–stretch data obtained from uniaxial tensile tests and investigated the relations between elastic modulus and in vivo RAC of proximal PAs with MRI and Echo techniques. We found that RAC is inversely related to the elastic modulus and that the RAC measured from both MRI and Echo correlates well to the elastic modulus.

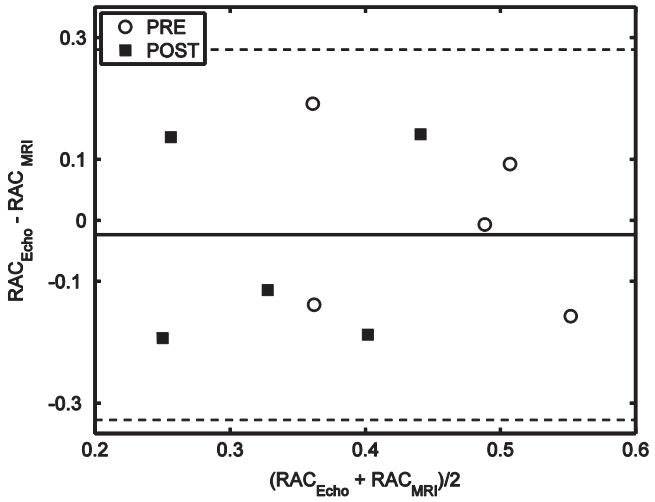

Fig. 2. Bland–Altman agreement analysis between the two measurements of RPA RAC via MRI and Echo. PRE and POST denote before and after acute embolization, respectively.

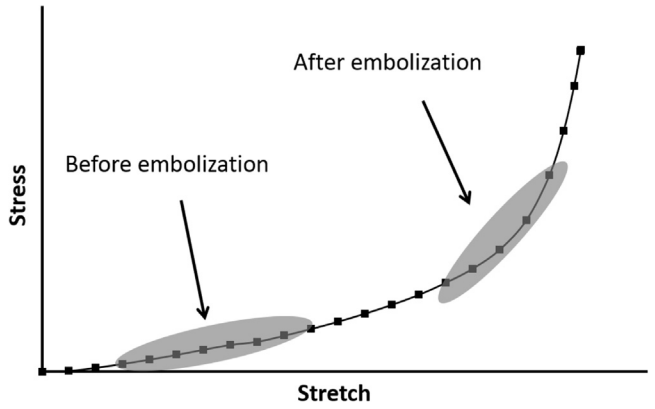

Fig. 3. A representative stress–stretch curve with physiological operating regions for before and after embolization indicated by gray ellipses.

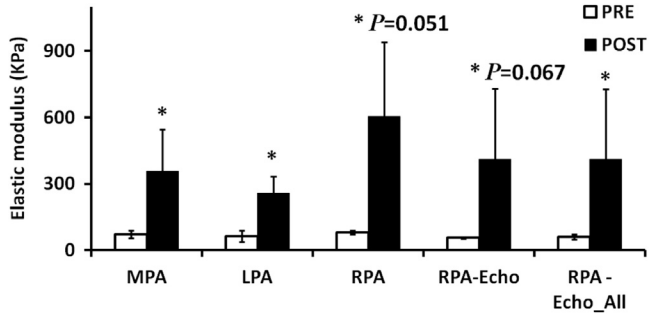

Fig. 4. Ex vivo elastic moduli (E_{ex}) of MPA, LPA, and RPA before (PRE) and after (POST) acute embolization. While the elastic modulus of all three PAs were estimated using the in vivo PA ID measured from MRI, the elastic modulus of RPA was also estimated using the PA ID measured from Echo as indicated in the figure, "RPA-Echo" ($n=5$ for PRE group only including female beagles) and "RPA-Echo_ALL" (n = 10 for PRE group including both male and female beagles). *$P < 0.05$ for POST vs. PRE. MPA: 358 ± 187 vs. 72 ± 16 kPa, $P=0.025$; LPA: 257 ± 77 vs. 64 ± 11 kPa, $P=0.03$; RPA via MRI: 603 ± 337 vs. 81 ± 9 kPa, $P=0.051$; RPA via Echo including female beagles only: 411 ± 318 vs. 57 ± 4 kPa, $P=0.067$; RPA via Echo including both female and male beagles: 411 ± 318 vs. 60 ± 11 kPa, $P=0.003$.

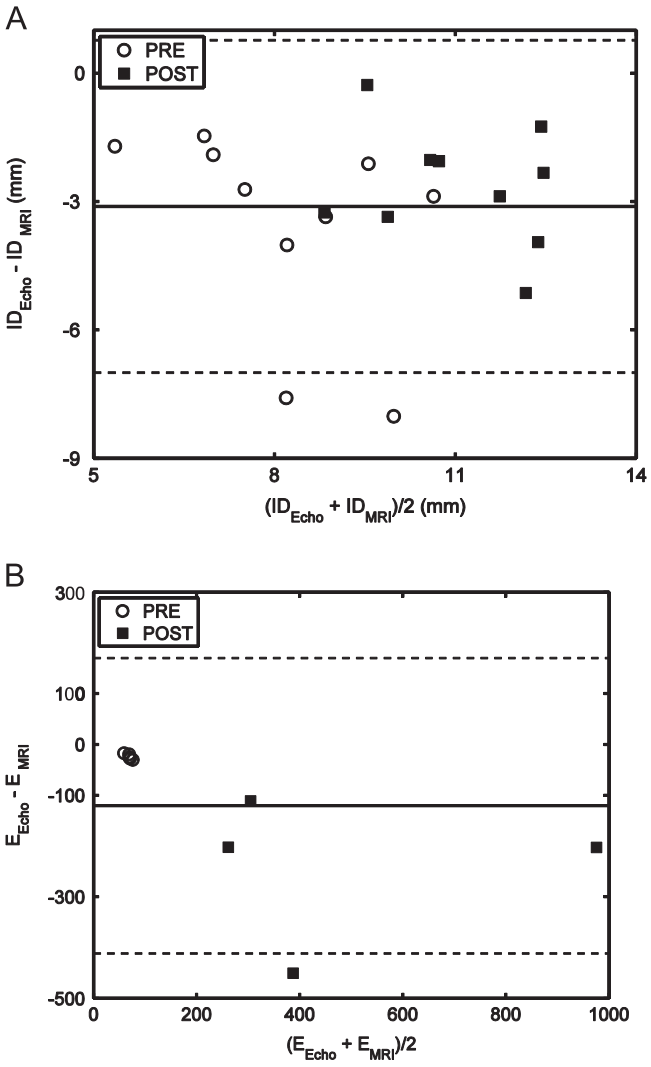

Fig. 5. Bland–Altman agreement analysis (A) between ID measured from MRI and Echo (B) between the calculated RPA ex vivo elastic modulus (E_{ex}) using the in vivo geometry data obtained via MRI and Echo. Note that in (B) 5 data points from PRE group are nearly coincident at the coordinate (~ 70, ~ -20). PRE and POST denote before and after acute embolization, respectively.

4.1. Elastic modulus

The stress–stretch curve is nonlinear or J-shaped (Fig. 3) with the elastin being the dominant mechanical component at low stretch and the collagen being the dominant mechanical component at high stretch (Kobs et al., 2005; Lammers et al., 2008; Roach and Burton, 1957; Tian et al., 2012). Before embolization, the

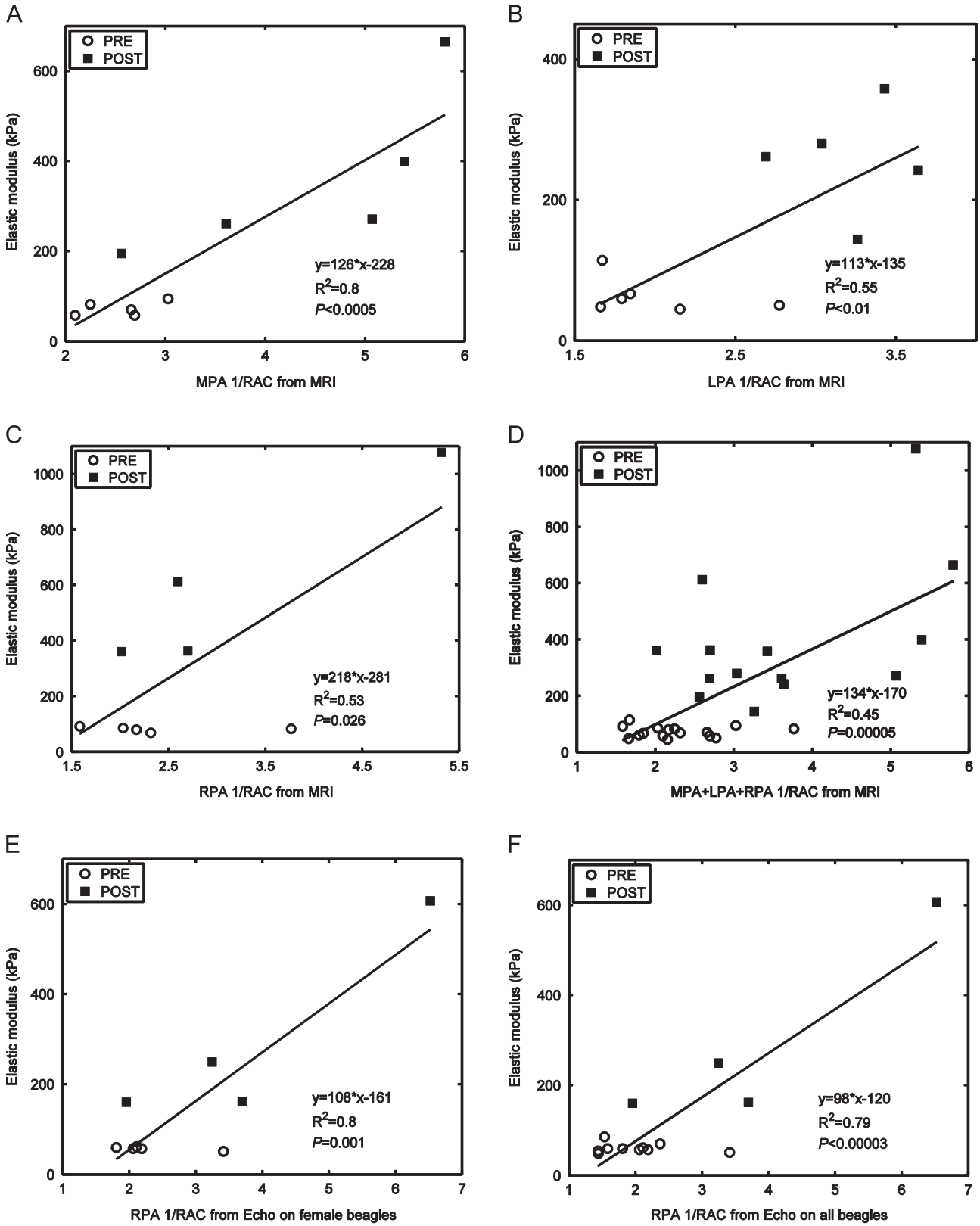

Fig. 6. Linear correlation between ex vivo elastic modulus (E_{ex}) and inverse relative area change (1/RAC) in (A) MPA, (B) LPA, (C) RPA, (D) MPA+LPA+RPA, (E) RPA-Echo, and (F) RPA-Echo_All with in vivo PA luminal area obtained from MRI for (A–D) all three PAs and Echo for (E) RPA_Echo with female beagles only and (F) RPA_Echo_All with both female and male beagles. PRE and POST denote before and after acute embolizations, respectively.

pressure is low and the stress and stretch are also low. As a result, in the physiological pressure–stretch–stress range, the artery was loaded in the elastin-dominant region and had a small elastic modulus (Fig. 3). After embolization, the pressure is high and the stress and stretch are also high, which shifted the pressure–stretch–stress range such that the artery was loaded in the collagen-dominant region and had larger elastic modulus (Fig. 3).

Although both male and female beagles were combined for this study, the RPA stress–stretch curves of these two groups are not significantly different (data not shown). Therefore, it is acceptable to combine the data from all these beagles for the correlation analysis between RAC and elastic modulus.

4.2. Correlation between elastic modulus and RAC

As shown in Figs. 3 and 4 the elastic modulus increased with acute embolization-induced PH, which corresponds to the decreased RAC with acute embolization-induced PH (Table 1). The inverse relationship between elastic modulus and RAC (Fig. 6) is expected for two reasons. First, RAC is the normalized change of area or stretch in the physiological state and describes the arterial distensibility under a certain pressure change. The elastic modulus is the change of stress over stretch and describes how strongly the artery resists deformation. As a result, a higher elastic modulus results in less distensibility, which should decrease RAC. Second, the stress–stretch curve of the three proximal PAs are J-shaped with an approximately linear region at low stretch, a transition region and another approximately linear region at high stretch. The relationship between the slope of this J-shaped curve (or the elastic modulus) and the stretch is also J-shaped with three regions. The relationship between slope and the change of stretch is then L-shaped. Since RAC is the normalized change of stretch, this L-shaped relationship indicates that the slope or elastic modulus (E_{ex}) is more likely linear to the inverse of RAC as shown in Eq. (4): $E_{ex}=(A/\mathrm{RAC})+B$.

A previous study on normoxic and hypoxic neonatal calves found only a moderate correlation between RAC and ex vivo elastic modulus in MPA ($R^2=0.48$; Hunter et al., 2010). However, we found a strong correlation in MPA ($R^2=0.80$; Fig. 6A). One reason for the difference could be the large difference in ages of the experimental animals, as the previous study was on newborn calves and this study was on adult beagles, especially given the dramatic changes that occur in the pulmonary circulation in the early post-natal period (Stenmark and Mecham, 1997). Also, the Hunter et al. study (Hunter et al., 2010) investigated a chronic change in pressure whereas our study imposed an acute change in pressure, which was therefore not accompanied by arterial remodeling. The increase in elastic modulus due to chronic hypoxia in neonatal calves was much smaller than that of the acute beagles in this study, which could be responsible for the weaker correlation in the neonatal calf study compared to ours. Nevertheless, a change in elastic modulus can occur due to remodeling, an increase in pressure (and thus stress), or both. Our study demonstrates that an increase in pressure alone can increase elastic modulus and thus decrease RAC.

4.3. MRI versus echo measurement of PA geometry and RAC

MRI measurement of in vivo PA geometry has been suggested to be more accurate than Echo measurement (Benza et al., 2008; Fakhri et al., 2012). However, MRI requires sedation, which can alter hemodynamics. Echo measurement, on the other hand, does not require sedation even for animal subjects. Our results show that there is little bias in the RPA RAC between Echo and MRI measurement (Fig. 2), and the RPA RAC calculated from either MRI or Echo measurement did not show a significant decrease after acute embolization (Table 1). Interestingly, the RPA cross-sectional area or ID measured via Echo is smaller than that measured via MRI (Fig. 5A) with two outliers probably because the ultrasound beam did not pass the RPA center. As a result, the elastic modulus of the RPA is consistently smaller using the geometry data measured via Echo than via MRI (Fig. 5B). This is especially true after acute embolization (Fig. 5B) because the elastic modulus is more sensitive to stretch at high stretch due to the J-shaped stress–stretch curve (Fig. 3). Nonetheless, significant correlation exists between RPA elastic modulus and in vivo RAC calculated from both Echo and MRI measurements (Fig. 6C, E and F).

Although it is difficult to obtain clear images from Echo measurement on MPA or LPA, the Echo measurement on RPA alone may be sufficient for most clinical applications. Indeed, previously RAC of RPA alone obtained by MRI has been found to predict mortality in patients with PAH (Gan et al., 2007). Therefore, Echo measurement is believed to be an acceptable method for measuring RAC to monitor the progression of PH.

4.4. Clinical application

Several clinical studies have focused on the relationship between RAC and PH severity (Gan et al., 2007; Stevens et al., 2012; Swift et al., 2012). However, RAC is actually a site-specific measure of proximal PAs and therefore should indicate the local properties. The proximal PAs have been shown to remodel in animal models of PH (Huang et al., 2001; Kobs et al., 2005; Lammers et al., 2008; Ooi et al., 2010; Tian et al., 2011; Wang et al., 2013), and the elastic modulus of proximal PAs have been speculated to be useful for clinical prognostics (Hunter et al., 2010). However, no studies have sought this correlation in an adult model of PH. A previous study examined the correlation between RAC and elastic modulus of MPA in a hypoxic neonatal calf model of PH (Hunter et al., 2010), but the post-natal period is one of dramatic changes in the PA mechanical properties (Stenmark and Mecham, 1997), so their findings may not apply to clinical adult PH. Our current study extended previous clinical and basic science studies by examining the relationship between RAC and elastic modulus of proximal PAs in the absence of remodeling and found that in all three proximal PAs (MPA, LPA and RPA) there is an inverse relationship between RAC and elastic modulus. Note that the acute PH created with embolization in this study is only clinically relevant to exercise-induced PH or acute high-altitude or hypoxia exposure. However, the absence of arterial remodeling in this model allowed us to better investigate the relationship between pressure, PA systolic and diastolic area and PA elasticity within a single stress–stretch curve. In addition, based on our current study, we speculate that such an inverse relationship also occurs in the case of chronic PH. This relationship could be useful for clinical application, because the predicted proximal PA stiffening from the change of RAC appears to occur earlier than the change of RV function (Stevens et al., 2012) and thus the proximal PA mechanical properties require attention for treatment. Indeed, treatments that address arterial stiffening have found success in systemic hypertension (Fleenor et al., 2012) and similar strategies may be effective in pulmonary hypertension.

4.5. Limitations

Several limitations are noted in this study. First, we were not able to measure the in vivo longitudinal stretch of MPA due to the MRI image quality and assumed the in vivo longitudinal stretch to be the average value of LPA. Since MPA and LPA are approximately aligned, this assumption is reasonable. Second, in the physiological condition both circumferential and longitudinal directions are loaded. Our uniaxial tensile test did not capture such loading condition. Biaxial testing or using a validated constitutive model could provide more accurate estimate of elastic modulus. Third, the smooth muscle cell activity was not considered in the estimation of the elastic modulus ex vivo.

5. Conclusion

We have shown that RAC is inversely related to the elastic modulus of proximal PAs in a canine model of acute embolization PH, and both MRI and Echo measurements are acceptable methods to obtain in vivo RAC of RPA. The established method will be employed in future studies that will investigate the changes of RAC and elastic moduli of proximal PAs in a chronic canine model of PH and the relations between these two parameters.

Conflict of interest statement

No conflicts of interest, financial or otherwise, are declared by the author(s).

Acknowledgments

This study was supported in part by National Institutes of Health (NIH) Grants R01-HL105598 (NCC), and funding support from Departments of Radiology (CJF) and Surgery (SHD) at the University of Wisconsin-Madison. L. Tian would like to thank Prof. Wendy C. Crone, Max Slick, Graham Fischer and Andrew Glaudell from the Department of Engineering Physics at the University of Wisconsin-Madison for assistance in performing mechanical testing on pulmonary artery tissues.

Appendix A. Supporting information

Supplementary data associated with this article can be found in the online version at: http://dx.doi.org/10.1016/j.jbiomech.2014.07.013.

References

Bellofiore, A., Roldán-Alzate, A., Besse, M., Kellihan, H.B., Consigny, D.W., Francois, C. J., Chesler, N.C., 2013. Impact of acute pulmonary embolization on arterial stiffening and right ventricular function in dogs. Ann. Biomed. Eng. 41, 195–204.

Benza, R., Biederman, R., Murali, S., Gupta, H., 2008. Role of cardiac magnetic resonance imaging in the management of patients with pulmonary arterial hypertension. J. Am. Coll. Cardiol. 52, 1683–1692.

Bland, J.M., Altman, D.G., 1986. Statistical methods for assessing agreement between two methods of clinical measurement. Lancet 1, 307–310.

Fakhri, A.A., Hughes-Doichev, R.A., Biederman, R.W.W., Murali, S., 2012. Imaging in the evaluation of pulmonary artery hemodynamics and right ventricular structure and function. Heart Fail. Clin. 8, 353–372.

Fleenor, B.S., Sindler, A.L., Eng, J.S., Nair, D.P., Dodson, R.B., Seals, D.R., 2012. Sodium nitrite de-stiffening of large elastic arteries with aging: role of normalization of advanced glycation end-products. Exp. Gerontol. 47, 588–594.

Gan, C.T.-J., Lankhaar, J.-W., Westerhof, N., Marcus, J.T., Becker, A., Twisk, J.W.R., Boonstra, A., Postmus, P.E., Vonk-Noordegraaf, A., 2007. Noninvasively assessed pulmonary artery stiffness predicts mortality in pulmonary arterial hypertension. Chest 132, 1906–1912.

Groves, B.M., Reeves, J.T., Sutton, J.R., Wagner, P.D., Cymerman, A., Malconian, M.K., Rock, P.B., Young, P.M., Houston, C.S., 1987. Operation Everest II: elevated high-altitude pulmonary resistance unresponsive to oxygen. J. Appl. Physiol. 63, 521–530.

Huang, W., Sher, Y.P., Delgado-West, D., Wu, J.T., Peck, K., Fung, Y.C., 2001. Tissue remodeling of rat pulmonary artery in hypoxic breathing. I. Changes of morphology, zero-stress state, and gene expression. Ann. Biomed. Eng. 29, 535–551.

Hunter, K.S., Albietz, J.A., Lee, P.-F., Lanning, C.J., Lammers, S.R., Hofmeister, S.H., Kao, P.H., Qi, H.J., Stenmark, K.R., Shandas, R., 2010. In vivo measurement of proximal pulmonary artery elastic modulus in the neonatal calf model of pulmonary hypertension: development and ex vivo validation. J. Appl. Physiol. 108, 968–975.

Hunter, K.S., Lee, P.-F., Lanning, C.J., Ivy, D.D., Kirby, K.S., Claussen, L.R., Chan, K.C., Shandas, R., 2008. Pulmonary vascular input impedance is a combined measure of pulmonary vascular resistance and stiffness and predicts clinical outcomes better than pulmonary vascular resistance alone in pediatric patients with pulmonary hypertension. Am. Heart J. 155, 166–174.

Hyduk, A., Croft, J.B., Ayala, C., Zheng, K., Zheng, Z.-J., Mensah, G.A., 2005. Pulmonary hypertension surveillance—United States, 1980–2002. MMWR. Surveill. Summ. 54, 1–28.

Kobs, R.W., Muvarak, N.E., Eickhoff, J.C., Chesler, N.C., 2005. Linked mechanical and biological aspects of remodeling in mouse pulmonary arteries with hypoxia-induced hypertension. Am. J. Physiol. Heart Circ. Physiol. 288, H1209–H1217.

Kornet, L., Jansen, J.R., Nijenhuis, F.C., Langewouters, G.J., Versprille, A., 1998. The compliance of the porcine pulmonary artery depends on pressure and heart rate. J. Physiol. 512, 917–926 (Part 3).

La Gerche, A., Heidbüchel, H., Burns, A.T., Mooney, D.J., Taylor, A.J., Pfluger, H.B., Inder, W.J., Macisaac, A.I., Prior, D.L., 2011. Disproportionate exercise load and remodeling of the athlete's right ventricle. Med. Sci. Sports Exerc. 43, 974–981.

Lammers, S.R., Kao, P.H., Qi, H.J., Hunter, K.S., Lanning, C., Albietz, J., Hofmeister, S., Mecham, R., Stenmark, K.R., Shandas, R., 2008. Changes in the structure-function relationship of elastin and its impact on the proximal pulmonary arterial mechanics of hypertensive calves. Am. J. Physiol. Heart Circ. Physiol. 295, H1451–H1459.

Lopez-Garcia, M.D.C., Beebe, D.J., Crone, W.C., 2010. Young's modulus of collagen at slow displacement rates. Biomed. Mater. Eng. 20, 361–369.

Mahapatra, S., Nishimura, R.A., Oh, J.K., McGoon, M.D., 2006. The prognostic value of pulmonary vascular capacitance determined by Doppler echocardiography in patients with pulmonary arterial hypertension. J. Am. Soc. Echocardiogr. 19, 1045–1050.

Motley, H.L., Cournand, A., 1947. The influence of short periods of induced acute anoxia upon pulmonary artery pressures in man. Am. J. Physiol. 150, 315–320.

Ooi, C.Y., Wang, Z., Tabima, D.M., Eickhoff, J.C., Chesler, N.C., 2010. The role of collagen in extralobar pulmonary artery stiffening in response to hypoxia-induced pulmonary hypertension. Am. J. Physiol. Heart Circ. Physiol. 299, H1823–H1831.

Roach, M.R., Burton, A.C., 1957. The reason for the shape of the distensibility curves of arteries. Can. J. Biochem. Physiol. 35, 681–690.

Roldán-Alzate, A., Frydrychowicz, A., Johnson, K.M., Kellihan, H., Chesler, N.C., Wieben, O., François, C.J., 2014. Non-invasive assessment of cardiac function and pulmonary vascular resistance in an canine model of acute thromboembolic pulmonary hypertension using 4D flow cardiovascular magnetic resonance. J. Cardiovasc. Magn. Reson. 16, 23.

Sanz, J., Kariisa, M., Dellegrottaglie, S., Prat-González, S., Garcia, M.J., Fuster, V., Rajagopalan, S., 2009. Evaluation of pulmonary artery stiffness in pulmonary hypertension with cardiac magnetic resonance. JACC. Cardiovasc. Imaging 2, 286–295.

Stenmark, K.R., Mecham, R.P., 1997. Cellular and molecular mechanisms of pulmonary vascular remodeling. Annu. Rev. Physiol. 59, 89–144.

Stevens, G.R., Garcia-Alvarez, A., Sahni, S., Garcia, M.J., Fuster, V., Sanz, J., 2012. RV dysfunction in pulmonary hypertension is independently related to pulmonary artery stiffness. JACC. Cardiovasc. Imaging 5, 378–387.

Swift, A.J., Rajaram, S., Condliffe, R., Capener, D., Hurdman, J., Elliot, C., Kiely, D.G., Wild, J.M., 2012. Pulmonary artery relative area change detects mild elevations in pulmonary vascular resistance and predicts adverse outcome in pulmonary hypertension. Invest. Radiol. 47, 571–577.

Tian, L., Lammers, S.R., Kao, P.H., Albietz, J.A., Stenmark, K.R., Qi, H.J., Shandas, R., Hunter, K.S., 2012. Impact of residual stretch and remodeling on collagen engagement in healthy and pulmonary hypertensive calf pulmonary arteries at physiological pressures. Ann. Biomed. Eng. 40, 1419–1433.

Tian, L., Lammers, S.R., Kao, P.H., Reusser, M., Stenmark, K.R., Hunter, K.S., Qi, H.J., Shandas, R., 2011. Linked opening angle and histological and mechanical aspects of the proximal pulmonary arteries of healthy and pulmonary hypertensive rats and calves. Am. J. Physiol. Heart Circ. Physiol. 301, H1810–H1818.

Wang, Z., Lakes, R.S., Eickhoff, J.C., Chesler, N.C., 2013. Effects of collagen deposition on passive and active mechanical properties of large pulmonary arteries in hypoxic pulmonary hypertension. Biomech. Model. Mechanobiol. 12, 1115–1125.